HIBISCUS PUBLISHER

JOURNAL OF ENVIRONMENTAL MICROBIOLOGY AND TOXICOLOGY

Website: http://journal.hibiscuspublisher.com/index.php/JEMAT/index

JEMAT VOL 8 NO 2 2020
Mathematical models

Mathematical Modeling of the Molybdenum Blue Production from *Serratia* sp. strain DRY5

Mohd Arif Syed[1], Nor Aripin Shamaan[2], Mohd. Yunus Shukor[1]*

[1]Department of Biochemistry, Faculty of Biotechnology and Biomolecular Sciences, Universiti Putra Malaysia, UPM 43400 Serdang, Selangor, Malaysia.
[2]Faculty of Medicine and Health Sciences, Universiti Sains Islam Malaysia, 55100 USIM, Kuala Lumpur, Malaysia.

*Corresponding author:
Prof. Dr. Mohd. Yunus Abd. Shukor
Department of Biochemistry,
Faculty of Biotechnology and Biomolecular Sciences,
Universiti Putra Malaysia, 43400 UPM Serdang,
Selangor,
Malaysia.
Email: yunus.upm@gmail.com

HISTORY

Received: 15th Nov 2020
Received in revised form: 15th Dec 2020
Accepted: 27th Dec 2020

KEYWORDS

molybdenum reduction
molybdenum blue
bioremediation
modelling
Serratia sp.

ABSTRACT

The reduction of molybdenum to molybdenum blue is a detoxification process and the development of Mo-blue is associated with growth. Significant parameters such as precise reduction rate, theoretical maximum reduction and whether reduction at high molybdenum concentration influenced the lag time of reduction can be discovered by mathematical modeling of the reduction phase. While common, the use of the linearization method by the use of natural logarithm transformation is inaccurate and can only provide an approximate value for the calculated single parameter, the real growth rate. In this work, a variety of models for such as logistic, Gompertz, Richards, Schnute, Baranyi-Roberts, Von Bertalanffy, Buchanan three-phase and more recently Huang were utilized to obtain values for the above parameters or constants. The Huang model was the best model in modelling the Mo-blue production curve of the *Serratia* sp. strain DRY5 based on statistical tests such as root-mean-square error (RMSE) (0.043), adjusted coefficient of determination (R^2) (0.994), bias factor (BF) (1.00), accuracy factor (AF) (1.03) and corrected AICc (Akaike Information Criterion) (-67.02). Parameters obtained from the fitting exercise were maximum Mo-blue production rate (μ_m), lag time (λ) and maximal Mo-blue production (Y_{max}). We make use of primary growth models for modeling Mo-blue output in this work. This is an emerging method of identifying constants of parameters that control the reduction of molybdenum. For the creation of further secondary models, the constants calculated from this work will be utilized for such purpose. The use of these primary models can also be broadened to processes involving the detoxification of other heavy metals.

INTRODUCTION

Molybdenum is a toxic heavy metal and its pollution worldwide has been reported in areas such as in Terengganu in Malaysia [1], the Tokyo Bay, Tyrol in Austria and in the Black Sea, where molybdenum level reaches worrying concentrations [2]. Furthermore, terrestrially, waste sludge contamination has been recognised as a major source of molybdenum pollutant that presents a health threat [2]. The source of these pollutions is due to the widespread use of molybdenum in industries such as alloying agent, anti-freeze part of the automotive engine, corrosion-resistant steel section and as molybdenum disulphide lubricant. At levels of several parts per million, molybdenum is very poisonous to ruminants, with cows is by far the most impacted [3,4]. A variety of Mo-reducing bacteria have been isolated to date, and several of these bacteria have also been locally identified [5–12,12,13] and several international strains from Egypt, Indonesia, Pakistan and Nigeria [14–25] and Antarctica [26–28]. In contrast with other heavy metals such as arsenic, selenium and chromium, the presumed low toxicity of molybdenum to humans and other animals has resulted in not many works as a detoxification procedure on molybdenum reduction. Nevertheless, newer research on molybdenum toxicity in spermatogenesis suppression and embryogenesis arrest in organisms such as catfish and rodents at levels as low as a few ppm has increased interest [29,30] and will spur more works on microbial molybdenum detoxification in the near future.

Molybdenum reduction to molybdenum blue is a mechanism related to bacterial growth and, similar to bacterial growth, also reveals a special stage in which the real growth rate starts at a value of zero, after which it hastens to a maximum

value (μ_{max}) producing a lag time (λ). In addition, growth curves require a final period in which the trend decreases and gradually reaches zero, at which, an asymptote (A) is reached. Adjustments in the growth rate frequently contribute to a sigmoidal curve with lag step features just after t = 0. This is accompanied by an exponential period, a stationary stage and then the process of death [31]. In addition to the asymptotic value and the lag time, the maximum specific growth rate (μ_m) is another useful growth curve parameter. This importance is also used in the creation of secondary models, such as the impact on the growth rate of the organism of the substrate, substance, pH and temperature. The μ_m is also given by the slope of the line considering that the logarithm of the activity or cellular microbial number is usually utilized, where the behavior increases or spreads exponentially [32].

A technique for obtaining this parameter is to calculate the slope of this curve by manually measuring the part of the curve which is roughly linear and then using linear regression. The most widely mentioned technique is the modification of natural logarithmic data by linearizing the sigmoidal curve. A slightly simpler approach is to describe the entire data group using a growth model of nonlinear regression and then estimate the μ_{max}, λ, and A from the model [33]. Moreover, the growth curve was created by several published works, but no further attempt was made to adapt the data to the available models.

Mathematical modelling of the Mo-blue production process have been explored previously [20,27,28,34,35]. That being said, the linearization of the Mo-blue output over time profile is used by both of these works to achieve the basic growth rate for further secondary modeling. The main model is also incomplete. Mathematical expressions regulating microbial processes such as development, inactivation or survival are discussed by the primary models. These activities are measured as ln (cell forming unit/ml), optical density, dry or wet weights, or other equivalent methods [36,37]. Secondary models cope with the effect or modification of primary model parameters due to changes in external stimuli or environmental factors such as temperature, water activity, pH, etc.

Hence, the objective of this work is to evaluate several available primary models such as Logistic [31,38], Gompertz [31,39], Richards [31,40], Schnute [31], Baranyi-Roberts [41], von Bertalanffy [42,43], Buchanan three-phase [36] and more recently Huang model [44] in modeling Mo-blue production from *Serratia* sp. strain DRY5, a molybdenum-reducing bacterium.

Materials and Methods

Mathematical models

Primary mathematical models such as modified logistic, modified Gompertz, modified Richards, modified Schnute, Baranyi-Roberts, von Bertalanffy, Buchanan three-phase and more recently Huang were utilized in this study (**Table 1**).

Isolation and maintenance of the Molybdate-reducing bacterium

The bacterium was previously isolated, identified and characterized by Rahman et al. [45]. The growth and maintenance was carried out on solid agar in low phosphate media (pH 7.0) containing glucose (1%), $(NH_4)_2SO_4$ (0.3%), $MgSO_4.7H_2O$ (0.05%), NaCl (0.5%), yeast extract (0.0.5%), $Na_2MoO_4.2H_2O$ (0.242%) and Na_2HPO_4 (0.071% or 5 mM) [45]. Glucose was separately autoclaved.

Preparation of resting cells for molybdenum reduction characterization

As previously developed, monitoring of Mo-blue output at different sodium molybdate concentrations was carried out statically using resting cells in a microplate or microtiter format. [46]. Cells was grown overnight in High Phosphate media (HPM) at room temperature on orbital shaker (150 rpm) with the phosphate concentration fixed at 100 mM. Cells harvesting was carried out by centrifugation at 15,000 x g for 10 minutes. Cellular suspension of 180 µL from a stock (A600 nm = 1.0) was sterically pipetted into each well of a sterile microplate. Various sodium molybdate concentrations in a volume of 20 µL from a stock solution was then added to each well to initiate Mo-blue production. The plates were then sealed and incubated statically at room temperature. Plate was read periodically at 750 nm (BioRad (Richmond, CA) Microtiter Plate reader (Model No. 680). The production of Mo-blue from the media in a microplate format was measured using the specific extinction coefficient of 11.69 $mM.^{-1}.cm^{-1}$ at 750 nm [47].

Table 1. Mo-blue production models used in this study.

Model	p	Equation
Modified Logistic	3	$y=\frac{A}{\left\{1+\exp\left[\frac{4\mu_m}{A}(\lambda-t)+2\right]\right\}}$
Modified Gompertz	3	$y=A\exp\left\{-\exp\left[\frac{\mu_m e}{A}(\lambda-t)+1\right]\right\}$
Modified Richards	4	$y=A\left\{1+v\exp(1+v)\exp\left[\frac{\mu_m}{A}(1+v)\left(1+\frac{1}{v}\right)(\lambda-t)\right]\right\}^{\left(\frac{-1}{v}\right)}$
Modified Schnute	4	$y=\left(\mu_m\frac{(1-\beta)}{\alpha}\right)\left[\frac{1-\beta\exp(\alpha\lambda+1-\beta-\alpha t)}{1-\beta}\right]^{\frac{1}{\beta}}$
Baranyi-Roberts	4	$y=A+\mu_m x+\frac{1}{\mu_m}\ln\left(e^{-\mu_m x}+e^{-h0}-e^{-\mu_m x-h_o}\right)-\ln\left(1+\frac{e^{\mu_m x+\frac{1}{\mu_m}\ln\left(e^{-\mu_m x}+e^{-h0}-e^{-\mu_m x-h0}\right)}-1}{e^{(y\max-A)}}\right)$
Von Bertalanffy	3	$y=K\left[1-\left[1-\left(\frac{A}{K}\right)^3\right]\exp^{-\left(\mu_m x/3K^{\frac{1}{3}}\right)}\right]^3$
Huang	4	$y=A+y\max-\ln\left(e^{A}+\left(e^{Y\max}-e^{A}\right)e^{-\mu_m B(x)}\right)$ $B(x)=x+\frac{1}{\alpha}\ln\frac{1+e^{-\alpha(x-\lambda)}}{1+e^{\alpha\lambda}}$
Buchanan Three-phase linear model	3	Y = A, IF X < LAG Y=A + K(X–λ), IF λ ≤ X ≥ X_{Max} Y = Y_{Max}, IF X ≥ X_{Max}

Note:
A= Mo-blue lower asymptote;
p= no of parameter
μ_m= maximum specific Mo-blue production rate;
v= affects near which asymptote maximum Mo-blue production occurs.
λ=lag time
y_{max}= Mo-blue upper asymptote;
e = exponent (2.718281828)
t = sampling time
α,β, k = curve fitting parameters
h_0 = a dimensionless parameter quantifying the initial physiological state of the reduction process. The lag time (h^{-1}) can be calculated as $h_0=\mu_{max}$

Determination of Kinetic Parameters for Molybdenum Blue production from *Serratia* sp. strain DRY5

Fitting of the data

Nonlinear regression was carried out to match the growth data to the nonlinear equations utilizing the Marquardt algorithm that minimizes sums of square of residuals utilizing CurveExpert Professional software (Version 1.6).

Statistical analysis

A variety of approaches have been statistically tested to determine if there is a statistically meaningful discrepancy between models with different number of parameters in terms of the consistency of fit to the same experimental results. including the corrected AICc (Akaike Information Criterion), Root-Mean-Square Error (RMSE), bias factor (BF), accuracy factor (AF), and adjusted coefficient of determination (R^2).

The RMSE was determined with reference to **equation 1**, where Ob_i is the experimental data, Pd_i are the values forecasted by the model, n is the number of experimental data and p is the number of parameters of the evaluated model. The model with the lower number of parameters is predicted to give lower RMSE values [48].

$$RMSE = \sqrt{\frac{\sum_{i=1}^{n}(Pd_i - Ob_i)^2}{n-p}} \qquad \textbf{(Equation 1)}$$

The determination coefficient or R^2 is used to determine the fit consistency of a model in linear regression. However, the use of the R^2 approach does not readily offer a comparable study where the variations in the number of parameters from one model and another vary. In order to solve this issue the adjusted R^2 is used (Equations 2 and 3), where S_y^2 is the total variance of the y-variable and RMS is Residual Mean Square.

$$Adjusted\ (R^2) = 1 - \frac{RMS}{s_Y^2} \qquad \textbf{(Equation 2)}$$

$$Adjusted\ (R^2) = 1 - \frac{(1-R^2)(n-1)}{(n-p-1)} \qquad \textbf{(Equation 3)}$$

The Akaike Knowledge Criterion (AIC) offers a modell selection solution to compute for almost every given experimental data the relative efficiency of a given statistical model. [49]. AIC handles the trade-off in regard to the goodness of fit of the model as well as the complexness of the model. It is in reality founded on information theory. The approach provides a comparative overview of the information lost in each model used to represent the information or data operation. The most approved model would be a model with the lowest value for AIC for the performance of a sequence of forecasted simulations. The corrected variant of AIC, the Akaike data criteria (AIC) with correction or AICc is used instead for data which have a smaller number of values or have a high number of parametres [50]. The AICc is calculated for each data set for each model according to the following equation (Eqn. 4);

$$AICc = 2p + n\ln\left(\frac{RSS}{n}\right) + 2(p+1) + \frac{2(p+1)(p+2)}{n-p-2} \qquad \textbf{(Equation 4)}$$

Where n represents the size of points in the curve and p is the number of parameters used in the formula. The technique takes the difference in fitness and the number of parameters in two models into account. The model with the lowest AICc value is generally more accurate for each data collection [50].

Accuracy Factor (AF) and Bias Factor (BF) to test for the goodness-of-fit of the models was calculated according to Eqns. 5 and 6 as suggested and first proposed by Ross [51]. A bias factor equal to 1 means that the values measured and expected fit preferably. For microbial growth curves or Mo-blue production studies, a bias factor having values < 1 signifies a fail-dangerous model whilst a bias factor having values > 1 signifies a model that is fail-safe. The value of the Accuracy Factor is usually ≥ 1, with higher AF values signifies prediction that is less precise or accurate.

$$\text{Bias factor} = 10^{\left(\sum_{i=1}^{n}\log\frac{(Pd_i/Ob_i)}{n}\right)} \qquad \textbf{(Equation 5)}$$

$$\text{Accuracy factor} = 10^{\left(\sum_{i=1}^{n}\log\frac{|(Pd_i/Ob_i)|}{n}\right)} \qquad \textbf{(Equation 6)}$$

RESULTS AND DISCUSSION

The production of Mo-blue from this bacterium was sigmoidal, lagging at about 15 hours and achieving the full production of Mo-blue at around 50 hours of static incubation (**Fig. 1**). The Mo-blue production fitted to eight different primary models is acceptable visually (**Fig. 2**). The best performance was Huang model with the best error function results such as smallest RMSE and AICc values. A value for adjusted R^2 nearest to unity. The AF and BF values were also excellent for the model with their values were the closest to 1.0. The poorest performance was Baranyi-Roberts with the lowest score for most of the statistics tests (**Table 2**). The coefficients for the Huang model at various molybdenum concentrations are shown in **Table 3**.

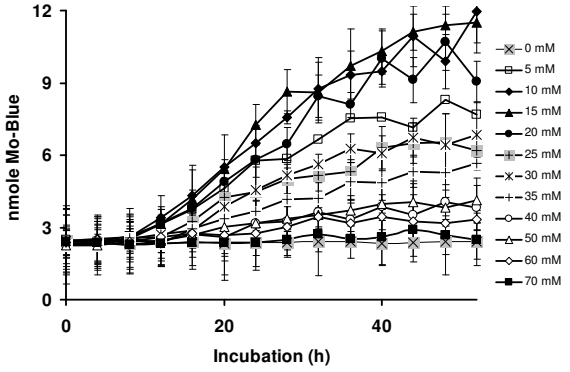

Fig. 1. The Mo-blue production curves of *Serratia* sp. strain DRY5 at various concentrations of sodium molybdate over time. The error bars represent mean ± standard deviation of three replicates.

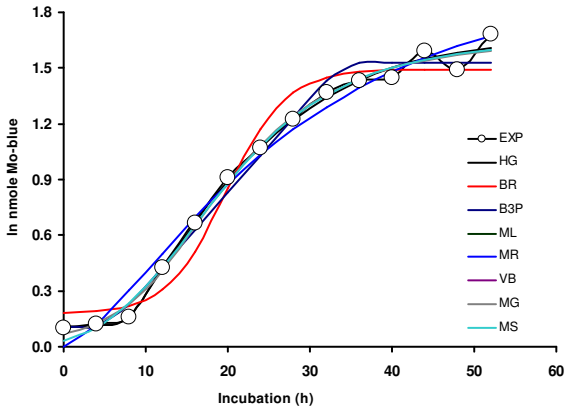

Fig. 2. The Mo-blue production curve of *Serratia* sp. strain DRY5 at 20 mM of sodium molybdate fitted to various models. The models utilized were Huang (HG), Baranyi-Roberts (BR), Buchanan-three phase (B3P), modified Logistics (ML), modified Richards (MR), von Bertalanffy (VB), modified Gompertz (MG) and modified Schnute (MS).

Table 2. Statistical analysis of the various fitted models.

Model	p	RMSE	adR2	AF	BF	AICc
Huang	4	0.043	0.994	1.031	1.000	-67.02
Baranyi-Roberts	4	0.120	0.951	1.196	1.061	-38.59
modified Gompertz	3	0.096	0.969	1.080	0.994	-50.56
Buchanan-3-phase	3	0.075	0.981	1.080	1.017	-57.32
modified Richards	4	0.085	0.976	6.796	0.169	-48.38
modified Schnute	4	0.111	0.959	1.146	0.938	-40.69
modified Logistics	3	0.062	0.987	1.096	1.033	-62.62
von Bertalanffy	3	0.058	0.989	1.670	0.636	-64.63

Note:
p no of parameters
adR^2 Adjusted Coefficient of determination
BF Bias factor
AF Accuracy factor

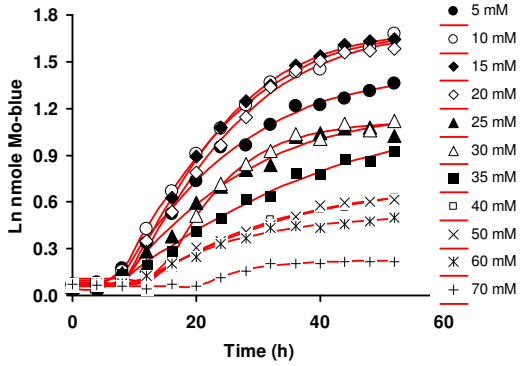

Fig. 3. The Mo-blue production curves of *Serratia* sp. strain DRY5 on various concentrations of sodium molybdate fitted using the Huang model (red line).

Table 3. Mo-blue production coefficients at various molybdenum concentrations as modelled using the Huang model.

Mo	Y_0	Lag (h)	Y_{max}	µmax (per h)
5 mM	0.08	6.839	1.42	0.08
10 mM	0.07	6.638	1.713	0.088
15 mM	0.092	8.661	1.699	0.1
20 mM	0.082	8.804	1.694	0.091
25 mM	0.061	7.133	1.179	0.072
30 mM	0.11	6	1.116	0.063
35 mM	0.04	5.872	1.18	0.064
40 mM	0.067	10.52	0.72	0.054
50 mM	0.07	11.29	0.697	0.046
60 mM	0.073	10.23	0.522	0.037
70 mM	0.062	21.21	0.222	0.027

In the model proposed by Huang [44,52], the first consideration is to describe the growth of a bacteria or increased in a growth –associated product with a 1st-order growth kinetics that does not take into account the lag and stationary phase yet. This can be described as follows;

$$\frac{dA}{dt}=\mu_m A \qquad \textbf{(Equation 7)}$$

A 1st-order kinetics growth of bacterium would show an exponentially increase activity or bacterial cells (**Equation 7**), the number of bacteria increases exponentially. The following expansion of the above Equation to smoothly modelled between the exponential and stationary phases is given in **Equation 8**. A_{max} is a maximum capacity that indicate the limits of bacterial growth or maximum cell density that is often reached at the stationary phase.

$$\frac{dA}{dt}=kA(A_{\max}-A) \qquad \textbf{(Equation 8)}$$

Where $kA_{max} = \mu_m$ when A is $\leq A_{max}$
The only problem with equation **Equation 8** is that it is only suitable for describing the growth curve but not the lag phase. A two-part model (**Equation 9**) is needed to describe all of the phases of growth that include the lag, exponential, and stationary phases.

$$\frac{dA}{dt}=0 \quad \text{if } t \leq \lambda,$$
$$\frac{dA}{dt}=kA(A_{\max}-A) \quad \text{if } t > \lambda, \qquad \textbf{(Equation 9)}$$

The entire process of growth from the lag to the stationary phases can be described by **Equation 10**. During the lag phase, the number of cells stays constant resulting in the value of *dA/dt* = 0. After this phase, an exponential growth of the bacterial growth started and is expressed in **Equation 10**. The problem with **Equation 10** is that it is a discontinuous model with 2 separate equations. Huang et al. introduce a unit step function (U) (also known as the Heaviside function after Oliver Heaviside) to describe the abrupt change between two transitional phases to glue the two equations together:

$$\frac{dA}{dt}=U(t-\lambda).kA(A_{\max}-A) \qquad \textbf{(Equation 10)}$$

The unit step function has a unique mathematical property of between 1 and 0. $U(t-\lambda)=0$ when $t \leq \lambda$ (within the lag phase). $U(t-\lambda) = 1$ when $t > \lambda$. Growth will be zero when $U(t-\lambda) = 0$. Bacterial growth follows ii when $U(t-\lambda) = 1$. The introduction of the unit step introduce another problem as it is a discrete function, and hence not continuous. In order to smoothen **Equation 10**, a smooth transitional unit function $f(t)$ is introduced by Huang et al.

$$\frac{dA}{dt}=kA(A_{\max}-A)f(t) \qquad \textbf{(Equation 11)}$$

where $f(t)$ represents the transitional function that describes the period of the lag phase. One such function is

$$\frac{dA}{dt}=\frac{1}{1+\exp[-\alpha(t-\lambda)]} \quad \textbf{(Equation 12)}$$

This mathematical property of this transitional function $f(t)$ is that if $t \leq \lambda$, $f(t) = 0$; and if $t \geq \lambda$, , $f(t) = 1$. The transitional function $f(t)$ will progressively alters from 0 to 1 when t approaches λ. The coefficient α defined the sharpness of the transition. The addition of $f(t)$ allows the description of the entire growth process as follows;

$$\frac{dA}{dt}=\frac{kA(A_{max}-A)}{1+\exp[-\alpha(t-\lambda)]} \quad \textbf{(Equation 13)}$$

This continuous differential growth equation (**Equation 13**) can be analytically solved using the method of variables separation. The ultimate general growth model is then depicted as follows:

$$y(t)=y_0+y_{max}-\ln\{\exp(y_0)+[\exp(y_{max})-\exp(y_0)]\exp[-k\exp(y_{max})B(t)]\}$$

Where

$$B(t)=t+\frac{1}{\alpha}\ln\frac{1+\exp[-\alpha(t-\lambda)]}{1+\exp(\alpha\lambda)} \quad \textbf{(Equation 14)}$$

The model identifies the duration of the lag phase (λ) rather clearly. The variables in the equation such as y_0, y_{max}, and $y(t)$, are identical to the parameters in the Baranyi model. The rate constant for the exponential phase in **Equation 7** has the unit of $(CFU/g \cdot time)^{-1}$, and is represented by the variable k. The transition factor is B(t), and the value of α in B(t) is the lag phase transition coefficient (LPTC). The transition coefficient (α) is in fact not easy to be determined from the growth curve by nonlinear regression especially so when data points from the lag phase is not enough. This coefficient specifies the transition from the lag phase towards the exponential phase. As a result, the transition coefficient was suggested arbritarily to be large enough (i.e. 25). When this is done, **Equation 14** becomes the full growth model that is continuous covering the entire range from the lag, exponential and to the stationary phase. The selection of α value as 25 allows the quick and smooth transition of the lag to the exponential phase of the growth curve. In addition, this allow the lag phase to be determined accurately. Furthermore, convergence of nonlinear regression using a few data points is also quick at this value.

The unit transitional function following the lag phase is equivalent to 1. When $t > \lambda$, the rate of growth will not be affected. Immediately following the lag phase bacterial growth would adhere to the relationship put together in **Equation 8**. Consequently, the bacterial growth maximum rate is obtainable using this equation. The establishment of the real-time growth rate in accordance with the natural logarithm of the bacterial number is as follows:

$$\mu=\frac{dy}{dt}=\frac{d[\ln(A)]}{dt}=\frac{1}{A}\frac{dA}{dt}=k(A_{max}-A) \quad \textbf{(Equation 15)}$$

At $A = A_0$, the bacterial count is minimal and maximum growth occurs. From here the maximum growth rate can be determined as follows;

$$\mu_m=k(A_{max}-A_0) \quad \textbf{(Equation 16)}$$

.

Parameters obtained from the fitting exercise were maximum Mo-blue production rate (μ_m), lag time (λ) and maximal Mo-blue production (Y_{max}). These biologically meaningful coefficients would be later used for secondary modelling of Mo-blue production using model such as the two-parameter Monod model or other more complex models "secondary models" such as Haldane, Aiba, Yano and others. In basic science, these mechanistic models are used to achieve a deeper understanding of the physical, chemical and biological mechanisms that relate to the growth profile that is observed. Mechanistic models are more efficient, all other things being equivalent, when they teach you about the fundamental mechanisms that drive trends. When extrapolating outside the observable parameters, they are more likely to function right [53].

CONCLUSION

Nonlinear regression using several primary models showed that the best model was Huang based on error function analysis. Parameters obtained from the fitting exercise are useful for secondary modelling in the future. Use of such bacterial growth models to reliably model Mo-blue output rates for further secondary model creation is novel, and this work has shown the application of such models, especially for the reduction of molybdenum to Mo-blue and for heavy metal detoxification processes generally. Current study involves secondary models of the production of Mo-blue from this bacterium in particular for its inhibitory impact on the overall Mo-blue production rate of these works. Furthermore, more secondary modeling studies are being performed on Mo-blue output speeds, including the influence of surrounding conditions (pH and temperature).

REFERENCES

1. Yakasai HM, Rahman MF, Yasid NA, Ahmad SA, Halmi MIE, Shukor MY. Elevated Molybdenum Concentrations in Soils Contaminated with Spent Oil Lubricant. J Environ Microbiol Toxicol. 2017 Dec 31;5(2):1–3.
2. Neunhäuserer C, Berreck M, Insam H. Remediation of soils contaminated with molybdenum using soil amendments and phytoremediation. Water Air Soil Pollut. 2001;128(1–2):85–96.
3. Underwood EJ. Environmental sources of heavy metals and their toxicity to man and animals. 1979;11(4–5):33–45.
4. Kincaid RL. Toxicity of ammonium molybdate added to drinking water of calves. J Dairy Sci. 1980;63(4):608–10.
5. Abo-Shakeer LKA, Ahmad SA, Shukor MY, Shamaan NA, Syed MA. Isolation and characterization of a molybdenum-reducing Bacillus pumilus strain lbna. J Environ Microbiol Toxicol. 2013;1(1):9–14.
6. Lim HK, Syed MA, Shukor MY. Reduction of molybdate to molybdenum blue by Klebsiella sp. strain hkeem. J Basic Microbiol. 2012;52(3):296–305.
7. Othman AR, Bakar NA, Halmi MIE, Johari WLW, Ahmad SA, Jirangon H, et al. Kinetics of molybdenum reduction to molybdenum blue by Bacillus sp. strain A.rzi. BioMed Res Int. 2013;2013.
8. Shukor MY, Ahmad SA, Nadzir MMM, Abdullah MP, Shamaan NA, Syed MA. Molybdate reduction by Pseudomonas sp. strain DRY2. J Appl Microbiol. 2010;108(6):2050–8.
9. Shukor MY, Habib SHM, Rahman MFA, Jirangon H, Abdullah MPA, Shamaan NA, et al. Hexavalent molybdenum reduction to molybdenum blue by S. marcescens strain Dr. Y6. Appl Biochem Biotechnol. 2008;149(1):33–43.
10. Shukor MY, Rahman MF, Shamaan NA, Syed MS. Reduction of molybdate to molybdenum blue by Enterobacter sp. strain Dr.Y13. J Basic Microbiol. 2009;49(SUPPL. 1):S43–54.
11. Shukor MY, Rahman MF, Suhaili Z, Shamaan NA, Syed MA. Hexavalent molybdenum reduction to Mo-blue by Acinetobacter calcoaceticus. Folia Microbiol (Praha). 2010;55(2):137–43.
12. Shukor MY, Rahman MF, Suhaili Z, Shamaan NA, Syed MA. Bacterial reduction of hexavalent molybdenum to molybdenum blue. World J Microbiol Biotechnol. 2009;25(7):1225–34.

13. Yunus SM, Hamim HM, Anas OM, Aripin SN, Arif SM. Mo (VI) reduction to molybdenum blue by Serratia marcescens strain Dr. Y9. Pol J Microbiol. 2009;58(2):141–7.
14. Campbell AM, Del Campillo-Campbell A, Villaret DB. Molybdate reduction by *Escherichia coli* K-12 and its chl mutants. Proc Natl Acad Sci U S A. 1985;82(1):227–31.
15. Gafasa MA, Ibrahim SS, Babandi A, Abdullahi N, Shehu D, Ya'u M, et al. Characterizing the Molybdenum-reducing Properties of *Pseudomonas* sp. locally isolated from Agricultural soil in Kano Metropolis Nigeria. Bioremediation Sci Technol Res. 2019 Jul 31;7(1):34–40.
16. Ibrahim Y, Abdel-Mongy M, Shukor MS, Hussein S, Ling APK, Shukor MY. Characterization of a molybdenum-reducing bacterium with the ability to degrade phenol, isolated in soils from Egypt. Biotechnologia. 2015;96(3):234–45.
17. Kabir ZM, Gafasa MA, Kabara HT, Ibrahim SS, Babandi A, M. Ya'u, et al. Isolation and Characterization of Molybdate-reducing *Enterobacter cloacae* from Agricultural Soil in Gwale LGA Kano State, Nigeria. J Environ Microbiol Toxicol. 2019 Jul 31;7(1):1–6.
18. Khan A, Halmi MIE, Shukor MY. Isolation of Mo-reducing bacterium in soils from Pakistan. J Environ Microbiol Toxicol. 2014;2(1):38–41.
19. Maarof MZ, Shukor MY, Mohamad O, Karamba KI, Halmi MIE, Rahman MFA, et al. Isolation and Characterization of a Molybdenum-reducing *Bacillus amyloliquefaciens* strain KIK-12 in Soils from Nigeria with the Ability to grow on SDS. J Environ Microbiol Toxicol. 2018 Jul 31;6(1):13–20.
20. Mansur R, Gusmanizar N, Dahalan FA, Masdor NA, Ahmad SA, Shukor MS, et al. Isolation and characterization of a molybdenum-reducing and amide-degrading *Burkholderia cepacia* strain neni-11 in soils from west Sumatera, Indonesia. IIOAB. 2016;7(1):28–40.
21. Mansur R, Gusmanizar N, Roslan MAH, Ahmad SA, Shukor MY. Isolation and characterisation of a molybdenum-reducing and Metanil yellow dye-decolourising *Bacillus* sp. strain Neni-10 in soils from West Sumatera, Indonesia. Trop Life Sci Res. 2017 Jan;28(1):69–90.
22. Masdor N, Abd Shukor MS, Khan A, Bin Halmi MIE, Abdullah SRS, Shamaan NA, et al. Isolation and characterization of a molybdenum-reducing and SDS- degrading *Klebsiella oxytoca* strain Aft-7 and its bioremediation application in the environment. Biodiversitas. 2015;16(2):238–46.
23. Mohammed S, Gafasa MA, Kabara HT, Babandi A, Shehu D, Ya'u M, et al. Soluble Molybdenum Reduction by *Morganella* sp. Locally-isolated from Agricultural Land in Kano. Bioremediation Sci Technol Res. 2019 Jul 31;7(1):1–7.
24. Saeed AM, El Shatoury E, Hadid R. Production of molybdenum blue by two novel molybdate-reducing bacteria belonging to the genus *Raoultella* isolated from Egypt and Iraq. J Appl Microbiol. 2019 Jun;126(6):1722–8.
25. Saeed AM, Sayed HAE, El-Shatoury EH. Optimizing the Reduction of Molybdate by Two Novel Thermophilic Bacilli Isolated from Sinai, Egypt. Curr Microbiol. 2020 May 1;77(5):786–94.
26. Ahmad SA, Shukor MY, Shamaan NA, Mac C, Syed MA. Molybdate reduction to molybdenum blue by an Antarctic bacterium. BioMed Res Int. 2013;2013:Article number 871941.
27. Rahman MF, Ahmad SA, MacCormack WP, Ruberto L, Shukor MY. Modelling the Effect of Copper on the Mo-reduction Rate of the Antarctic Bacterium *Pseudomonas* sp. strain DRY1. J Environ Microbiol Toxicol. 2017 Jul 31;5(1):21–5.
28. Rahman MFA, Yasid NA, Ahmad SA, Shamaan NA, Shukor MY. Characterization of molybdenum-reduction by an acrylamide-degrading Antarctic bacterium. In 10-3 Midori-cho, Tachikawa, Tokyo, Japan: National Institute of Polar Research (NIPR); 2018. Available from: http://id.nii.ac.jp/1291/00015258/
29. Yamaguchi S, Miura C, Ito A, Agusa T, Iwata H, Tanabe S, et al. Effects of lead, molybdenum, rubidium, arsenic and organochlorines on spermatogenesis in fish: Monitoring at Mekong Delta area and in vitro experiment. Aquat Toxicol. 2007;83(1):43–51.
30. Zhang Y-L, Liu F-J, Chen X-L, Zhang Z-Q, Shu R-Z, Yu X-L, et al. Dual effects of molybdenum on mouse oocyte quality and ovarian oxidative stress. Syst Biol Reprod Med. 2013;59(6):312–8.
31. Zwietering MH, Jongenburger I, Rombouts FM, Van't Riet K. Modeling of the bacterial growth curve. Appl Environ Microbiol. 1990;56(6):1875–81.
32. Fujikawa H. Development of a new logistic model for microbial growth in foods. Biocontrol Sci. 2010;15(3):75–80.
33. Johnsen AR, Binning PJ, Aamand J, Badawi N, Rosenbom AE. The Gompertz function can coherently describe microbial mineralization of growth-sustaining pesticides. Environ Sci Technol. 2013;47(15):8508–14.
34. Halmi MIE, Ahmad SA, Syed MA, Shamaan NA, Shukor MY. Mathematical modelling of the molybdenum reduction kinetics in Bacillus pumilus strain Lbna. Bull Environ Sci Manag. 2014;2(1):24–9.
35. Shukor MS, Shukor MY. Bioremoval of toxic molybdenum using dialysis tubing. Chem Eng Res Bull. 2015;18(1):6–11.
36. Buchanan RL. Predictive food microbiology. Trends Food Sci Technol. 1993;4(1):6–11.
37. Whiting RC. Modeling bacterial survival in unfavorable environments. J Ind Microbiol. 1993;12(3–5):240–6.
38. Ricker, F.J. 11 Growth Rates and Models. In: W.S. Hoar DJR and JRB, editor. Fish Physiology [Internet]. Academic Press; 1979 [cited 2014 Jun 27]. p. 677–743. (Bioenergetics and Growth; vol. Volume 8). Available from: http://www.sciencedirect.com/science/article/pii/S1546509808600345
39. Gompertz B. On the nature of the function expressive of the law of human mortality, and on a new mode of determining the value of life contingencies. Philos Trans R Soc London. 1825;115:513–85.
40. Richards, F.J. A flexible growth function for empirical use. J Exp Bot. 1959;10:290–300.
41. Baranyi J. Mathematics of predictive food microbiology. Int J Food Microbiol. 1995;26(2):199–218.
42. Babák L, Šupinová P, Burdychová R. Growth models of Thermus aquaticus and Thermus scotoductus. Acta Univ Agric Silvic Mendel Brun. 2012;60(5):19–26.
43. López S, Prieto M, Dijkstra J, Dhanoa MS, France J. Statistical evaluation of mathematical models for microbial growth. Int J Food Microbiol. 2004;96(3):289–300.
44. Huang L. Optimization of a new mathematical model for bacterial growth. Food Control. 2013;32(1):283–8.
45. Rahman MFA, Shukor MY, Suhaili Z, Mustafa S, Shamaan NA, Syed MA. Reduction of Mo(VI) by the bacterium Serratia sp. strain DRY5. J Environ Biol. 2009;30(1):65–72.
46. Shukor MS, Shukor MY. A microplate format for characterizing the growth of molybdenum-reducing bacteria. J Environ Microbiol Toxicol. 2014;2(2):42–4.
47. Shukor MY, Lee CH, Omar I, Karim MIA, Syed MA, Shamaan NA. Isolation and characterization of a molybdenum-reducing enzyme in Enterobacter cloacae strain 48. Pertanika J Sci Technol. 2003;11(2):261–72.
48. Motulsky HJ, Ransnas LA. Fitting curves to data using nonlinear regression: a practical and nonmathematical review. FASEB J Off Publ Fed Am Soc Exp Biol. 1987;1(5):365–74.
49. Akaike H. New look at the statistical model identification. IEEE Trans Autom Control. 1974;AC-19(6):716–23.
50. Burnham KP, Anderson DR. Model Selection and Multimodel Inference: A Practical Information-Theoretic Approach. Springer Science & Business Media; 2002. 528 p.
51. Ross T, McMeekin TA. Predictive microbiology. Int J Food Microbiol. 1994;23(3–4):241–64.
52. Huang L. Growth kinetics of Escherichia coli O157:H7 in mechanically-tenderized beef. Int J Food Microbiol. 2010;140(1):40–8.
53. Bolker BM. Ecological Models and Data in R. Princeton, N.J: Princeton University Press; 2008. 408 p.